iJRASET
International Journal For Research in Applied Science and Engineering Technology

# INTERNATIONAL JOURNAL FOR RESEARCH

IN APPLIED SCIENCE & ENGINEERING TECHNOLOGY

**Volume:** 6 **Issue:** II **Month of publication:** February 2018

**DOI:** http://doi.org/10.22214/ijraset.2018.2049

www.ijraset.com

Call: 08813907089 | E-mail ID: ijraset@gmail.com

International Journal for Research in Applied Science & Engineering Technology (IJRASET)
*ISSN: 2321-9653; IC Value: 45.98; SJ Impact Factor : 6.887*
*Volume 6 Issue II, February 2018- Available at www.ijraset.com*

# Comparative Photocatalytic Degradation of Rose Bengal Dye under Visible Light by $TiO_2$, $TiO_2$/PAni and $TiO_2$/PAni/GO Nanocomposites

Azad Kumar[1], Gajanan Pandey[2]
[1,2]*Department of Applied Chemistry, School of Physical Science Babasaheb Bhimrao Ambedkar University, Lucknow*

***Abstract:*** ***Nanocomposites of $TiO_2$, $TiO_2$/PAni and $TiO_2$/PAni/GO were prepared by in situ oxidation polymerization method. The prepared $TiO_2$, $TiO_2$/PAni and $TiO_2$/PAni/GO Nanocomposites were characterized by the XRD, SEM, TEM, BET, UV-Vis, FTIR, Band gap energy and Photolumiscence. The XRD confirmed the presence of Anatase and rutile phase in the prepared photocatalysts. The average particle size was found 68, 15 and 12 nm for $TiO_2$,$TiO_2$/PAni and $TiO_2$/PAni/GO respectively. The SEM and TEM images also confirmed the formation of nanocomposites in the range of ~ 100 nm. The surface area 37.52, 76.68 and 96.24$m^2$/g were observed for $TiO_2$, $TiO_2$/PAni and $TiO_2$/PAni/GO Nanocomposites respectively. The Band gap energy of $TiO_2$,$TiO_2$/PAni and $TiO_2$/PAni/GO were calculated by talc plot and obtained 3.0, 2.98 and 1.76 eV respectively. The Photocatalytic degradation of Rose Bengal dye was done at different condition viz concentration of dye, time of illumination, pH and dose of photocatalyst. The maximum photo degradation were found at neutral pH, 6.25 ppm concentration of dye solution, 800 mg/L amount of photocatalyst and 120 min irradiation of visible light. Kinetics of photo degradation was investigated for Rose Bengal dye and found first order kinetics. The coating of PAni and GO were enhanced the photocatalytic activity of Titania. Hence $TiO_2$/PAni and $TiO_2$/PAni/GOare the efficient photocatalyst for the degradation of Rose Bengal dye than pure $TiO_2$.***

***Keyword: Photocatalyst, Photo degradation, Rose Bengal, photocatalysis, nanocomposites, visible light irradiation, Photolumiscence.***

## I. INTRODUCTION

In recent years, due to industrialization, there is rapid increase in release of pollutants from industries into water bodies [1].The major source of environmental pollution is the wastewater effluent of textile industries. The textile industries are using the very large amount of chemically stable dyes which are causing water pollution. About 12% of dyes are used in textile industries in each year. During the synthesis and processing, about 20% dyes are lost in the environment such as Rose Bengal, Caramine, Rhodamine, Indigo Red, Thymol blue, Red 120, Eriochrome Black-T (EBT), Methylene Blue [2, 3]. Textile industries effluents contain colour pigments which are causing the carcinogenic effect on the human being and also causing serious impact on aquatic life. There are lots of dyes used in the textile industries. The xanthene dyes are mostly used in textile industries. Xanthene dyes can be characterized by the presence of xanthenes nucleus with aromatic groups as chromophore [4, 5]**.** Rose Bengal is a significant xanthene dye and widely used in textile and photochemical industries whose molecular structure as shown in Figure 1**.** Rose Bengal shows the severe toxic effects on the human health and also affects the corneal epithelium [6]. It is very hazardous for the human being because it causes the irritation, itchiness, blistering and reddening. It also affects on human eyes like eye redness, inflammation, itching etc. [8]. There are several, physical and chemical methods have been studied to remove the organic dyes such as Rose Bengal, Methylene blue etc. from the wastewater. The Physical techniques like photo degradation, coagulation**,** flocculation, reverse osmosis, adsorption on the activated carbon, ion exchange method and ultra-filtration, have been used to reduce the toxic effects of dye effluents. Furthermore, various chemical methods like photosensitized oxidation, adsorption, photo Fenton's reactions are also employed for removal of dyes. These techniques are not effective to remove the trace amount of dye from the waste water. Therefore we need green technology through which we can remove the dyes from the waste water. The photocatalytic degradation is the very advanced oxidation process to remove the dye without any side product formation.

Titanium dioxide ($TiO_2$) is the most used photocatalyst due to its non-toxicity, high activity, photostability, chemical stability, biological inertness, the good absorption, desorption rate of reactants and low cost [4]. $TiO_2$ photocatalyst has been applied to self-cleaning glasses, antibacterial tiles *etc*. as it has the strong oxidizing power to decompose most organic compounds to $CO_2$ [5].

Organic compounds such as halogeno-aliphatic hydrocarbons, halogeno aromatic hydrocarbons, organic acids, coloring matters, nitroaromatic hydrocarbons, substituted anilines, multi-ring aromatic hydrocarbons, hydroxybenzenes, surface active agents, and pesticides can be changed into non-toxic, decoloured inorganic compounds and ultimately eliminated as pollutants [6].

It is very interesting fact that $TiO_2$ absorbs only 5% UV portion of the solar light spectrum. There are two issues namely, limitation of light absorption by $TiO_2$ in the UV portion of the solar light spectrum and recombination of the electron (e-) - hole (h+) pairs. Several researches have been done to synthesized modified nanocomposites for the utilization of solar light [9]. Consequently, hundreds of $TiO_2$ variants and other oxide/non-oxides have been developed and tested in proposed to overcome the recombination process [10]. It is believed that availability of visible light absorbing photocatalysts would largely solve the technological problems photo reactor considerations. Additionally, harnessing sunlight can be achieved by the scientists recently, most of the researchers have used conducting polymers to modify $TiO_2$ to improve visible light photoactivity and electron transfer performance; e.g., Polyaniline/$TiO_2$ [11], polypyrrole/ $TiO_2$ [12] and polythiophene/$TiO_2$ [13]. Many published reports focussed on the preparation and photocatalytic studies on nanocomposites consisting of polyaniline and $TiO_2$ (PAni/$TiO_2$) [14-17]. Among these, PAni has several advantageous features over others because of its good environmental stability, ease of synthesis, controllable doping/dedoping chemistry, and reversible electrical properties by controlled charge transfer processes [18, 19].The incorporation of inorganic nanomaterials into PAni, thereby forming nanocomposite materials, appears to be an effective approach for preparing photocatalytic materials [20]. Some study reported that by adding graphene to PAni, there is an increase in the electric double-layer capacitance as well as charge transfer and charge transport [21]

In this study, the nanocomposites of $TiO_2$, $TiO_2$/PAni and $TiO_2$/PAni/GO were prepared by the co-deposition oxidation method. The prepared materials were characterized by the XRD, BET, TEM, SEM, UV-Vis, Band gap energy, Photoluminescence spectra, and FTIR. The prepared materials were used as photocatalyst for the photo degradation of Rose Bengal dye in the visible light. The photodegradation of Rose Bengal has been done at different chemical parameters i.e. pH of the solution, the concentration of dye, the amount of photocatalyst, photocatalyst, time of irradiation and recyclability of the photocatalyst. The kinetic study of photodegradation has been performed and found the order of reaction.

## II. METHODS AND MATERIALS

All the materials and chemicals used in the study were analytical grade and purchase from Merck without further purification.

### *A. Synthesis of Titanium Dioxide*

$TiO_2$ nanoparticles were prepared using $H_2O_2$ solution added to 10 ml of 1 mol/L ethanol solution of titanium tetra-isopropoxide (TTIP). Ethanol was added to the brown colored solution obtained, and the total volume of the solution was adjusted to 100 ml. The solution was then heated at 120°C for 1hr in a closed vessel. The solution was filtered and obtained the solid material, further it was washed with double distilled water 2 to 3 time and dry in the oven at 60 °C for 24 h. The obtained solid was calcined at 600°C for 3hr to get white titanium oxide powder [22-23].

### *B. Synthesis of $TiO_2$/PAniNanocomposite*

The synthesis of the $TiO_2$/PAninanocomposite was done by using aniline, TTIP as the $TiO_2$ precursor and Ammonium per sulfate as the oxidizing agent. In a typical process, 10 mL of $CCl_4$ and 4.0 mL of TTIP were placed in a beaker to which 1 mL of aniline were added. The entire system was stirred constantly on an ice bath. To the above dispersion of aniline, the solution of oxidant (0.5 M APS in 500 mL of 1M HCl) was added drop-wise, which simultaneous initiated the polymerization of aniline and the synthesis of $TiO_2$. The reaction mixture soon turned into the greenish black slurry, which was filtered after 2 hours, and washed sequentially with an excess of water and acetone to remove the excess APS and PAniOligomers. The synthesized $TiO_2$/Paninanocomposite was then de-doped with a 1M ammonia solution to neutralize the remaining acid, which converted the $TiO_2$/PAninanocomposite to its emeraldine base (EB) form. To render it conductive, the EB of $TiO_2$/PAninanocomposite was doped with 100 mL of 1M HCl solution for 12 hours, later filtered and dried in an air oven at 80 °C for 24 hours. Pure PAni was prepared in a similar manner but in the absence of TTIP. [24-25].

### *C. Synthesis of $TiO_2$/PAni/GONanocomposite*

The synthesis of the $TiO_2$/PAninanocomposite was done by using aniline, TTIP as the $TiO_2$ precursor and Ammonium per sulphate as the oxidizing agent. In a typical process, 10 mL of $CCl_4$, 4.0 mL of TTIP and 60 mg of prepared Graphene oxide were placed in a beaker to which 1 mL of aniline were added. The entire system was stirred constantly on an ice bath. To the above dispersion of

aniline, the solution of oxidant (0.5 M APS in 500 mL of 1M HCl) was added drop-wise, which simultaneous initiated the polymerization of aniline and the synthesis of $TiO_2$. The reaction mixture soon turned into greenish black slurry, which was filtered after 2 hours, and washed sequentially with an excess of water and acetone to remove the excess APS and PAni oligomers. The synthesized Pani-$TiO_2$nanocomposite was then de-doped with a 1M ammonia solution to neutralize the remaining acid, which converted the $TiO_2$/PAninanocomposite to its emeraldine base (EB) form. To render it conductive, the EB of $TiO_2$/PAninanocomposite was doped with 100 mL of 1M HCl solution for 12 hours, later filtered and dried in an air oven at 80 °C for 24 hours.

### *D. Characterizations*

The prepared $TiO_2$, /PAni, TiO2/PAni and TiO2/PAni/GO nanocomposites were characterized by x-ray diffraction (XRD) patterns in the range of 2θ = 20–80°. The size of $TiO_2$ particles was investigated with transmission electron microscope (TEM). The morphology of $TiO_2$, $TiO_2$/PAni and $TiO_2$/PAni/GO nanocomposites were investigated by scanning electron microscopy. Fourier-transform infrared (FTIR) was used for the bonding determination, UV-visible DRS was used for band gap energy determination and Photoluminescence was used for the hydroxyl radical mechanism determination and $e^-$-$h^+$ recombination determination.

### *E. Irradiation Procedure*

The dye and photocatalyst suspension were stirred in the dark for 30 min to reach adsorption equilibrium with the nanocomposites ($TiO_2$, /PAni, $TiO_2$/PAni and $TiO_2$/PAni/GO) surface. Irradiation experiments of dyes were carried out on stirred aqueous solutions contained in a 100 mL beaker. Degradations were performed on 20 mL of aqueous solutions containing the desired concentration of Rose Bengal. The amount of nanocomposites material varies from 100 mg/L to 800 mg/L. Irradiations were carried out using one UV-365 nm, Hanovia lamp (450 W). At any given irradiation time interval, the dispersion was sampled (5 mL), centrifuged, and subsequently filtered through a Millipore filter to separate the $TiO_2$ particles and take UV- Vis spectra to determine the residual concentration [26].

### *F. Determination of Hydroxyl Radicals*

To determine whether reactive oxygen species involved in the photocatalytic degradation of dyes is hydroxyl radical or not, terephthalic acid photoluminescence probing technique was used. In this, alkaline solution of terephthalic acid, having $TiO_2$, $TiO_2$/PAni and $TiO_2$/PAni/GO nanocomposites was irradiated with visible light. After 30 min of irradiation, a sample was withdrawn from the reaction mixture and was centrifuged to separate photocatalyst particles. The photoluminescence spectrum of the sample was recorded between 335 and 600 nm at an excitation wavelength of 325 nm and variation in the intensity of the peak at 425 nm was monitored using Perkin Elmer LS 55 Fluorescence Spectrometer [27].

## III. RESULTS AND DISCUSSION

### *A. Characterisation*

1) *XRD:* The XRD patterns of $TiO_2$, PAni, $TiO_2$/PAni, $TiO_2$/PAni/GO nanocomposite are showing in Fig 1. The XRD pattern of $TiO_2$ showing in Fig. 1(a) a series of characteristic peaks: 2θ = 25.32° (101), 37.86° (103), 48.06° (200), 55.09° (211) and 62.75° (204) are observed due to the tetragonal anatase phase of $TiO_2$ (JCPDS file No: 86-1157). Fig.1 (b) showing the XRD pattern of PAni, a broad peak corresponding to the periodicity parallel to the polymer chain to (200) plane was observed at 19.26° 2θ [28]. The peak at 2θ ~25° due to the periodicity perpendicular to the polymer chain and other crystal planes at 2θ ~15° was absent, which shows that the as-synthesized PAni is highly amorphous in nature. In the XRD pattern of the $TiO_2$/PAninanocomposites (Fig. 1c) the usual broad peak corresponding to the periodicity parallel to the polymer chain encompassing a slight crystalline small peak at 20° 2θ was not observed. All the peaks corresponding to anatase $TiO_2$ were also present. In the XRD pattern of the $TiO_2$/PAni/GO nanocomposites (Fig. 1d), all the peaks corresponding to anatase $TiO_2$ were also present suggesting that the state of $TiO_2$ did not change during the polymerization process. On the other hand, a slight reduction in the peak intensity and red shift was observed for $TiO_2$ peaks in the $TiO_2$/PAninanocomposite [29]. This might be due to the surface coating of PAni on $TiO_2$ during the polymerization process and the interactions between the $TiO_2$ nanoparticles and the PAni chain [30].

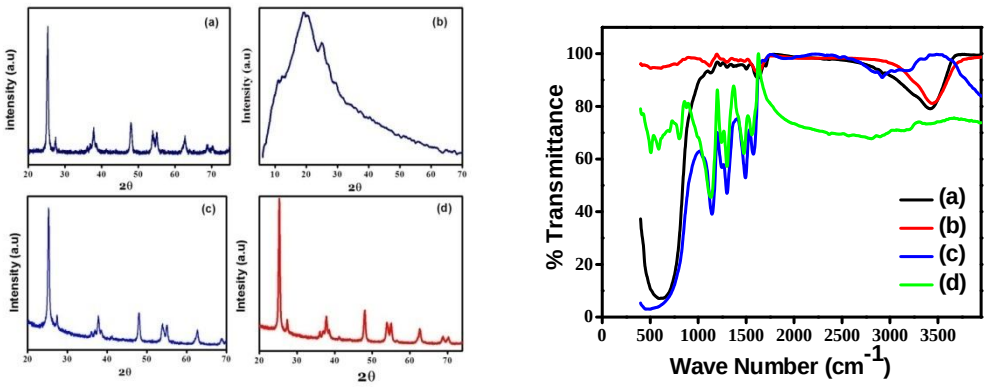


Fig.1 XRD Pattern and FTIR spectra of (a) $TiO_2$ (b) PAni (c) $TiO_2$/PAni (d) $TiO_2$/PAni/GO

2) *FTIR:* FT-IR spectra of $TiO_2$, PAni, $TiO_2$/PAni and $TiO_2$/PAni/GO are shown in Figure 3. In Figure 1(a), five peaks are observed due to O-Ti-O bond stretching (3418, 1628, 1502, 1302 and 1231 $cm^{-1}$) the main characteristic bands of polyaniline were seen in Figure 1b. The band at 3439 cm-1 is attributable to N-H stretching. Also the band at 1663 $cm^{-1}$ assigned to N-H bend of a primary aromatic amine. The peaks at 1484 and 1419 $cm^{-1}$ belong to C-C stretch in the ring and N-O asymmetric and 1219 $cm^{-1}$ C-O stretching and this confirms the presence of PAni and GO in the $TiO_2$/PAni/GO nanocomposite. Because titanium is a transition metal, it has intense tendency to form coordination compound with the nitrogen atom in PAni Macromolecule. This interaction may weaken the bond strengths of N-H, C=C, and C-O in PAni Macromolecule. These results confirm the presence of PAni and GO in nanocomposite [31].

3) *Scanning Electron Microscopy (SEM):* The morphology of the prepared nanocomposites was investigated by scanning electron microscopy and it resumes the most interesting outcomes. Fig.2 (a, b, c and d) clearly show that all the prepared nanocomposites are obtained in nanodiamension which is agglomerate form. The $TiO_2$, PAni, $TiO_2$/PAni and $TiO_2$/PAni/GO are indicating that the particle morphology is in spherical shape and disc shape. The $TiO_2$ molecule is agglomerate with PAni to form chips like structures which are partially spherical and disc shape. The nanocomposites were found to be in nanometerrange Fig.4 showing the $TiO_2$/PAni morphology which is in nanodiamension with little change in surface morphology. Fig.2 d showing the SEM image of $TiO_2$/PAni/GO which is in nanodiamension and the surface morphology of $TiO_2$/PAni/GO has been changed slightly, due to the coating of PAni and GO layer on the $TiO_2$ lattice. The surface of $TiO_2$/PAni/GO was observed like disk shape and spherical [32, 33].

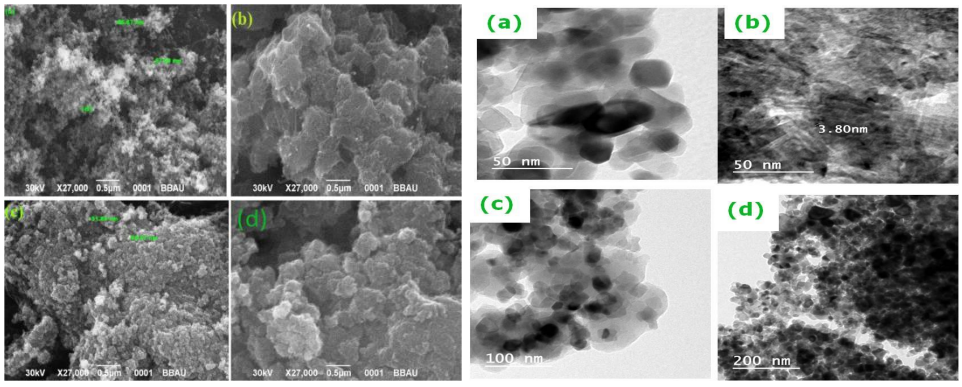


Fig.2 SEM and TEM images of (a) $TiO_2$ (b) PAni (c) $TiO_2$/PAni (d) PAni/$TiO_2$/GO

4) *TEM Analysis:* The TEM images of $TiO_2$, $TiO_2$/PAni and $TiO_2$/PAni/GO are shown in Fig 2. In the TEM of $TiO_2$ hexagonal crystal lattice structure has been observed (Fig.2a). Fig.5b showed the TEM image of pure polyaniline. In the TEM images, the spiral chain structure of PAni has been observed. From the TEM images, we find that PAni-modified $TiO_2$ does not change the size of $TiO_2$ significantly (Fig.2c). The sizes of both modified and $TiO_2$ are monodisperse about 10–20 nm. Moreover, the crystal lattice line can be clearly found in the TEM images. The aggregations of both kinds of particles are caused by high surface energy; however, the agglomeration of the modified one is alleviated obviously compared with that of the neat $TiO_2$[34, 35]. Generally, PAni synthesized by a chemical oxidative method in hydrochloric acid solution is the emeraldine salt (ES) form

(Fig. 2), only which is electrically conducting. Anatase $TiO_2$ nanoparticles were deposited by PAni (ES) so as to avoid $TiO_2$ particles agglomeration because the positive charges exclude each other.

5) *Brunauer-Emmett-Teller (BET) Surface Area Analysis:* Nitrogen adsorption–desorption isotherms were used to determine the structural characteristics and surface area of $TiO_2$, $TiO_2$/PAni and TiO2/PAni/GO nanocomposite. The $N_2$ adsorption-desorption isotherms of the $TiO_2$, $TiO_2$/PAni and TiO2/PAni/GO nano-composite were measured at 77 K, as shown in Figure 6. The specific surface areas (from BET and Surface area, pore volume and the pore radius of the $TiO_2$, $TiO_2$/PAni and $TiO_2$/PAni/GO nanocomposite are showing in Table 1. The surface area was found 37.52, 76.68 and 96.24 $m^2/g$ for $TiO_2$, $TiO_2$/PAni and $TiO_2$/PAni/GO respectively. There is an increase in pore volume (Vp) of $TiO_2$, $TiO_2$/PAni and $TiO_2$/PAni/GO nanocomposite and pore radius is decreased [36-38].

From these results, it may be concluded that the high surface area of the $TiO_2$/PAni/GO nanocomposite may favour rapid electron transport and high ion diffusion, allowing improved photochemical performance. Moreover, the BET surface areas increased remarkably in the $TiO_2$/PAni/GO nanocomposite, which suggests that $TiO_2$ is well intercalated in PAni matrix and may also provide direct conduction pathway for electrons. The formation of $TiO_2$ with PAni by co-deposition oxidation synthesis resulted in the generation of well dispersed $TiO_2$ in PAni Matrix giving one $TiO_2$/PAni system with a unique set of properties [39].

Table 1:- The specific surface area, pore volume and pore radius of the $TiO_2$, $TiO_2$/PAni and $TiO_2$/PAni/GO

| Sample | Surface area ($m^2/g$) | Pore volume ($cm^3/g$) | Pore radius (nm) |
|---|---|---|---|
| $TiO_2$ | 37. 523. | 1321.84 | |
| $TiO_2$/PAni | 76.68 | 6.51241.64 | |
| $TiO_2$/PAni/GO | 96.24 | 9.51241.21 | |

6) *UV-Vis spectrophotometer:* The absorption spectrum of $TiO_2$ consists of a single broad intense absorption around 263 nm (shown in Fig.3) in the region of the hypsochromic shift. The PAni (Fig.3b) showed absorbance in the shorter wavelength region about 225 nm while $TiO_2$/PAni results showed a red shift in the absorption onset value and the broad peak observed at 287 nm. This due to the coating of PAni layer on the surface of Titania [40]. The red shift that is observed at 298 nm in the absorption spectra with the decrease in particle size has been reported in $TiO_2$/PAni/GO nanocomposite. This is due to the coating of PAni and Graphene oxide in the Titania and the Titania completely interacted with PAni and GO.

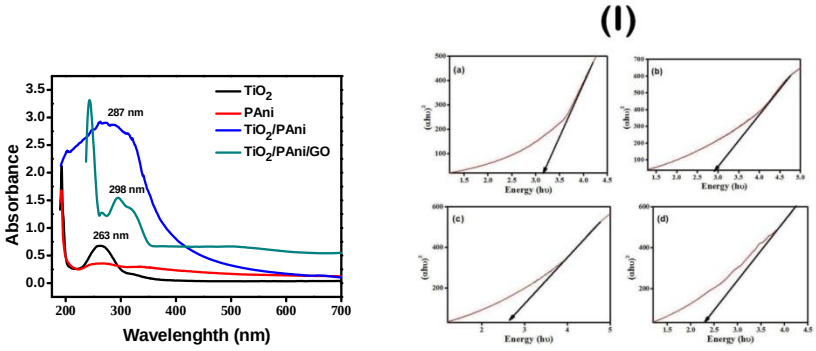


Fig.3. UV spectra of $TiO_2$, PAni, $TiO_2$/PAni, $TiO_2$/PAni/GO

7) *Determination of Optical Band Gap energy of composites:* The band gap of $TiO_2$, $TiO_2$/PAni and $TiO_2$/PAni/GO were determined from absorption spectra and Tauc relation (Eq. (2))

$$\alpha hv = B(hv - E_{gap})m \qquad (2)$$

The band gap energy of prepared materials was calculated by extrapolation of the $(\alpha hv)^2$ versus $hv$ plots, where $\alpha$ is the absorption coefficient and $hv$ is the photon energy, $hv = (1239/\lambda)$ eV. The value of $hv$ extrapolated to $\alpha = 0$ gives an absorption energy, which

corresponds to a band gap (*E*g) (showing in Fig.3). Graph yields an *E*g value of 3.2 eV for $TiO_2$ and 2.98 for $TiO_2$/PAni [41]. The slight decrease in band gap energy in case of $TiO_2$/PAni is due to the formation of sub-band level between the valence band and the conduction band. In the case of $TiO_2$/PAni/GO the band gap energy 1.74 eV was observed due to the coating of PAni and GO on the surface of Titania. In the other word, the PAni and GO form a subband in the Titania [42].

*B. Photodegradation*

The photo-catalytic degradation of Rose Bengal in the presence of $TiO_2$, $TiO_2$/PAni and $TiO_2$/PAni/GO nanocomposites has been studied. The solutions of dye were prepared in 10:1 (V/V) ratio of water and alcohol. The known amount of photocatalyst 100 mg/L to 1600 mg/L was dispersed in the dye solution. The reaction mixture was illuminated under visible light, while kept continuously under agitation, for the different time intervals and different concentration. The residual concentration of dye in the reaction mixture was measured spectrophotometrically. The results obtained for the degradation of Rose Bengal is shown in Fig.4 and 5.

Photocatalytic degradation efficiencies (h) are obtained by using following equation.

where $RB_0$ is the initial absorbance and $RB_F$ is the final sampled absorbance.

1) *Effect of Irradiation time:* The effect of the irradiation time on photodegradation of RB dye has been studied in presence of $TiO_2$, $TiO_2$/PAni and TiO2/PAni/GO nanocomposite. The UV spectrum has been taken for $TiO_2$, $TiO_2$/PAni and $TiO_2$/PAni/GO nanocomposite at different irradiation time (30, 60, 90, 120 and 180 min) (Fig. 4). It is interesting to remark that the absorbance decreases with the increase of time with the photocatalyst. At 120 minutes the photodegradation efficiency observed was 14, 93 and 97 % for $TiO_2$, $TiO_2$/PAni and $TiO_2$/PAni/GO nanocomposite respectively. The Titania was showed very low photodegradation efficiency in visible light. This is due to the high band gap energy (3.2 eV) which is not active in the visible light region. Whereas $TiO_2$/PAni and $TiO_2$/PAni/GO nanocomposite show very high photodegradation efficiency 93 and 97 %, this is due to the formation of sub-band in Titania. The coating of PAni and GO decrease the band gap energy of Titania and Titania becomes active in visible light [43].

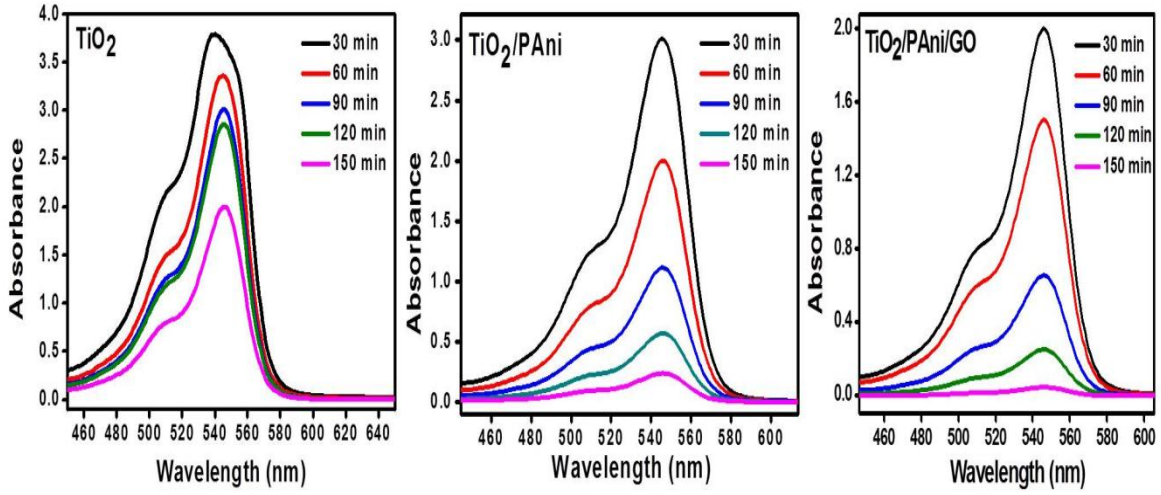


Fig.4 UV spectrum showing the effect of irradiation time on photodegradation with $TiO_2$, $TiO_2$/PAni and TiO2/PAni/GO nanocomposite

2) *Effect Of Photocatalyst:* The effect of photocatalyst was investigated. It is clear from the results shown in Fig.5 that $TiO_2$, $TiO_2$/PAni and $TiO_2$/PAni/GO nanocomposites are proving as an effective photocatalyst for the degradation of Rose Bengal dye. However, $TiO_2$/PAni/GO seems to be more effective as the photocatalyst for the degradation of Rose Bengal. The prominent degradation of Rose Bengal was found in 120 min study in the presence of $TiO_2$/PAni/GO in comparison to the prepared $TiO_2$ and $TiO_2$/PAni. This is due to the coating of polyaniline of Titania surface which provides the electron from the HOMO to LUMO. The electrons of HOMO get excited into LUMO which is further jumping into the conduction band of Titania [44].

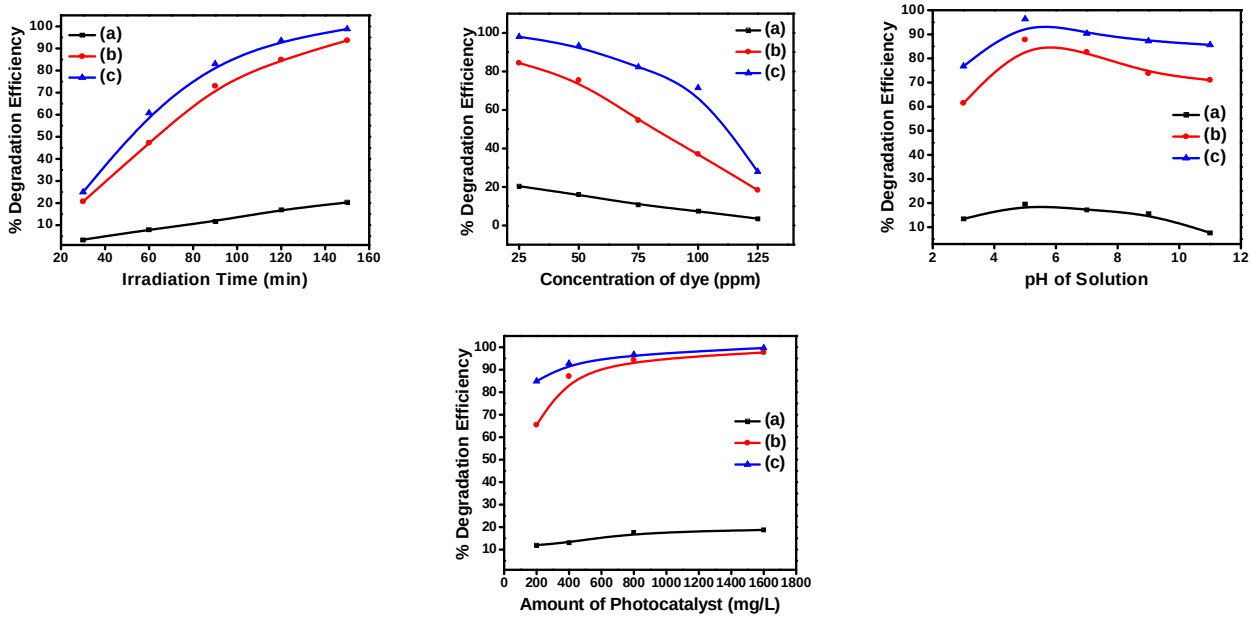


Fig. 5Photodegradation of Rose bengal at different parameters with(a) $TiO_2$, (b) $TiO_2$/PAni and (c) TiO2/PAni/GO

3) *Effect of concentration of dye:* The effect of dye concentration Keeping the catalyst loading concentration constant at 800 mg/L of the dye solution, the effect of varying concentration of the dye was studied on its rate of degradation (25, 50, 75, 100 and 125 ppm) as given in Fig.5. The rate of photodegradation was decreased with increasing concentration of RB. This is because as the number of dye molecules increase, the amount of light (quantum of photons) penetrating into the dye solution to reach the catalyst surface is reduced owing to the hindrance in the path of light. Thereby the formation of the reactive hydroxyl and superoxide radicals is also simultaneously reduced. Thus there should be an optimum value maintained for the catalyst and the dye concentration, wherein maximum efficiency of degradation can be achieved [45, 46].
4) *Effect of Ph:* The photodegradation was carried out under varying pH conditions from (3 to 11), by adjusting with $H_2SO_4$ and NaOH, with $TiO_2$ kept at constant amounts of photocatalyst of 800 mg/ L and 25 ppm concentration of dye solutions (Fig. 5). The photodegradation was found to have highest rates at neutral ranges of pH. While at lower pH it was found to decrease. In the basic condition, the photodegradation rate was found slow and very poor degradation.. Fig. 5 Effect of pH of solution on photodegradation of Rose Bengal with photocatalyst Hence highly acidic and basic condition is not encouraging for the degradation of rose bengal. This implies that neutral conditions are good towards the formation of the reactive intermediates that is hydroxyl radicals is significantly enhanced, which further help in enhancing the reaction rate. On the other hand in basic and acidic conditions, the formation of reactive intermediates is relatively less favourable and hence less spontaneous [47-48].
5) *Effect of photocatalyst Amount:* It is clear from the results shown in Fig.14 that $TiO_2$, $TiO_2$/PAni and $TiO_2$/PAni/GO nanocomposites are proving as an effective photocatalyst for the degradation of rose bengaldyes. The photodegradation of Rose Bengal was increasing with increases the amount of photocatalyst. It is observed that $TiO_2$/PAni/GO is the more effective photocatalyst than $TiO_2$ and $TiO_2$/PAni [44]. When the photocatalyst amount increases, the number of active site increase for the reaction of dyes. The amount of photocatalyst increases two times the rate of photodegradation increase about 30% and 60 %, in presence of $TiO_2$, $TiO_2$/PAni and $TiO_2$/PAni/GO respectively [49].

*C. Recyclability of Photocatalyst*

The recyclability of photocatalyst has been studied. The photocatalyst and Rose Bengal mixture was agitated, illuminated with visible light and after desired time, the mixture was centrifuged to remove the photocatalyst. The obtained photocatalyst washed three times with distilled water and finally kept in the oven for 24 h at 60 $^oC$ temperature and further it is reuse for the degradation of Rose Bengal. The photodegradation of Rose Bengal by the recyclizedPhotocatalyst are showing in Fig. 6. The result shows that the recyclizedphotocatalyst efficiency is decreasing due to the loss of some active sites and decrease of the collection efficiency of photon [50, 51].

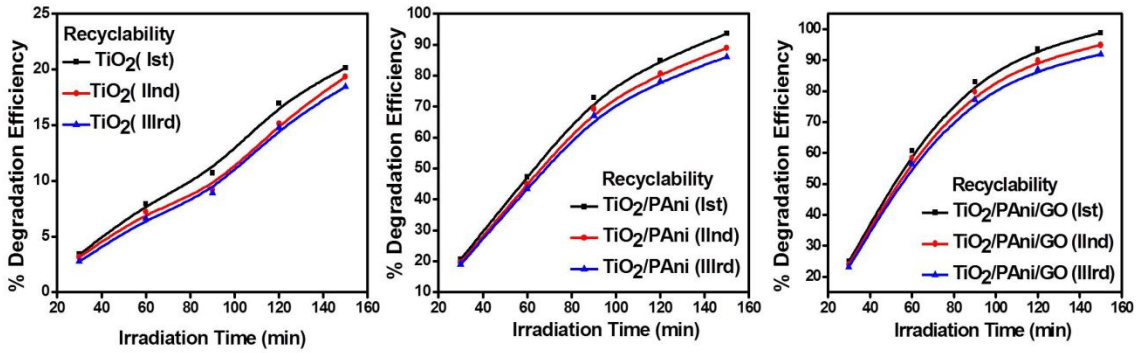


Fig.6. Photodegradation of Rose Bengal by Photocatalyst and recyclable Photocatalyst$TiO_2$, $TiO_2$/PAni, $TiO_2$/PAni/GO

*D. Lowering of electron-hole recombination*

Photoluminescence spectra have been utilized to look at the mobility of the charge carriers to the surface and in addition, the recombination process required by the electron-hole pair in semiconductor particles. PL emission comes about because of the radiative recombination of energized electrons and holes. It is a basic need of a decent photocatalyst to have least electron-hole recombination. To concentrate the recombination of charge carriers, PL investigations of incorporated materials have been attempted. PL emission intensity is directly related to recombination of excited electrons and holes. Fig. 7 shows the photoluminescence spectra of synthesized photocatalysts. It means $TiO_2$ and $TiO_2$/PAniwith strong PL intensity has high recombination of charge carriers where as$TiO_2$/PAni/GO has weak intensity. The weak PL intensity of $TiO_2$/PAni/GO may arise due to the coating of polyaniline on Titania lattice. The photo excited electrons were trapped into the graphene oxide. This delays the electrons- holes recombination process and hence is utilized in the redox reaction leading to improved photocatalytic activity [52, 53].

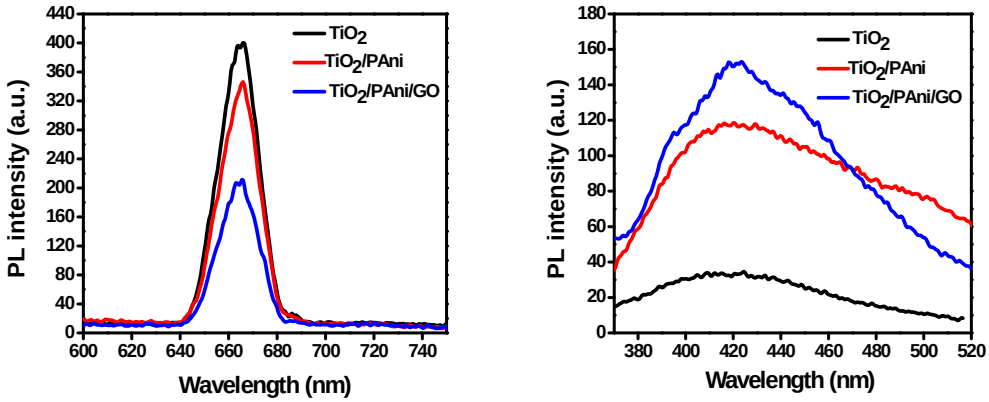


Fig.7Photolumiscence Spectra of $TiO_2$, $TiO_2$/PAni and $TiO_2$/PAni/GO Fig.8 PL spectra of photocatalyst with terephthalic acid (0.001M) $TiO_2$, $TiO_2$/PAni and $TiO_2$/PAni/GO

*E. Hydroxyl radical formation*

As the hydroxyl radical plays important role in the decomposition of the organic pollutants. It is important to explore the measure of hydroxyl radicals created by each photocatalyst. In this way, there is a strategy to build up the arrangement of hydroxyl radicals utilizingterephthalic acid (TA) as a probe molecule. In this technique, TA was reacting with OH radical forming 2-hydroxyl terephthalic acid (TAOH) which gives fluorescence peak at 426 nm. Fig. 8 denoted the fluorescent signal of all the photocatalysts after reacting with TA arrangement. The fluorescent intensity is linearly related to the number of hydroxyl radicals formed by the photocatalysts. It implies higher is the formation of hydroxyl radical, yield of TAOH will be high and subsequently more intense will be the fluorescence peak. Thus, $TiO_2$/PAni/GO with highest intensity confirms the generation more number of hydroxyl radicals compared to other photocatalysts. The fluorescence intensity follows the trend (i,e. $TiO_2$, < $TiO_2$/PAni< $TiO_2$/PAni/GO) of photocatalytic performance of all the photocatalyst [54, 55].

*F. Kinetics of photodegradation*

For the kinetic study of photocatalytic degradation, a control experiment was first carried out under two conditions, viz (i) dye + Visible light (no catalyst) (ii) catalyst+ dye in dark without any irradiation (Fig. 9). It can be seen that under dark conditions, the amount of dye adsorbed on the surface of photocatalyst becomes constant after 20 min, where the adsorption equilibrium is achieved with all the nanocomposites [58].

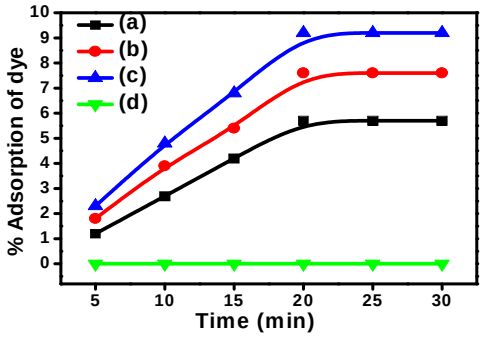


Fig.9 % Adsorption under dark condition (a) $TiO_2$ (b) $TiO_2$/PAni (c) $TiO_2$/PAni/GO (d) Dye + visible light without photocatalyst

The Langmuir-Hinshelwood kinetic model [59, 60] is widely used to describe the kinetics of photodegradation of many organic compounds. According to this model the degradation rate *r* of the dye is described as:

$$\mathbf{r} = -\frac{\mathbf{d[RB]}}{\mathbf{dt}} = -\frac{\mathbf{kK[RB]}}{\mathbf{1+K[RB]}} \quad (2)$$

Where *r* is the rate of degradation of RB, *k* is the rate constant, [RB] is the dyeconcentration, and *K* is the adsorption coefficient. The implicit solution is given in Eq.(3) :

$$\mathbf{ln}\frac{\mathbf{[RB]}}{\mathbf{[RB]_o}} + \mathbf{k}\,(\mathbf{[RB]} - \mathbf{[RB]o}]) = -\mathbf{kKt} \quad (3)$$

This can be solved explicitly for t by using discrete changes in [RB] from the initial concentration to a zero reference point. The model presented in Eq. (3) yields an exact solution for the degradation of RB. However, when the concentration of RB is very small in the ppm range, a pseudo-first-order model can be assumed, ignoring *K* [RB] in the denominator of eq. (2) leads to Eq. (4) :

$$\mathbf{r} = -\frac{\mathbf{d[RB]}}{\mathbf{[RB]}} = \mathbf{kK[RB]} = \mathbf{K'[RB]} \qquad \mathbf{(4)}$$

Integration of eq. (4) yields eq. (5)

$$\mathbf{[RB]} = \mathbf{[RB]}o\ \mathbf{e^{-K't}} \mathbf{(5)}$$

$$\mathbf{ln}\ \frac{\mathbf{[RB]}}{\mathbf{[RB]o}} = \mathbf{kKt} = \mathbf{K't} \mathbf{(6)}$$

Where *k*' is the pseudo rate constant and is in units of time$^{-1}$. Figure 20 shows the ln [$RB_o$-RB] *vs.* time plots for $TiO_2$, $TiO_2$/PAni and $TiO_2$/PAni/GO nanocomposite. Samples were dispersed in the same concentration of dye solutions. Pseudo-first-order degradation rate constants *k*' calculated from the slopes of Fig. 10 [61-62]. The rates constant were found 6.5x10$^{-3}$, 20.9x10$^{-3}$ and 30.5x10$^{-3}$ for the $TiO_2$, $TiO_2$/PAni and $TiO_2$/PAni/GO nanocomposite respectively.

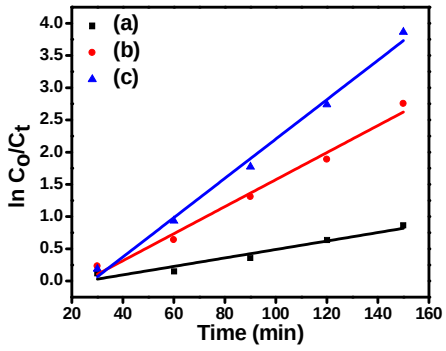


Fig.10 kinetics of photodegradation of RB with (a) $TiO_2$ (b) $TiO_2$/PAni (c) $TiO_2$/PAni/GO

## III. CONCLUSION

In this study, nanocomposites materials were prepared by the insitu co-deposition oxidative methods. Different techniques were used for the characterisation of the $TiO_2$, $TiO_2$/PAni and $TiO_2$/PAni/GO nanocomposite such as XRD, BET, SEM, TEM, FTIR, Photoluminescence, band gap energy and UV spectrophotometer. The XRD confirmed the presence of anatase and rutile phase were observed in the prepared materials nanocomposites. The SEM study confirms that spherical morphology of the nanocomposite. The TEM analysis confirms that the size of the nanocomposite. The FTIR characterization confirms that the $TiO_2$/PAni/GO molecules are well combined with polyaniline and graphene oxide structure. EDEX confirms about the elements which are present in the prepared sample by x-ray emission spectrum. The surface area 37.52, 76.68 and 96.24 $m^2/g$ were observed for $TiO_2$, $TiO_2$/PAni and $TiO_2$/PAni/GO Nanocomposites respectively. The Band gap energy of $TiO_2$, $TiO_2$/PAni and $TiO_2$/PAni/GO were calculated by tauc plot and obtained 3.0, 2.86 and 1.76 eV respectively. The Photocatalytic degradation of Rose Bengal dye was done at different condition viz concentration of dye, time of illumination, pH, and the dose of the photocatalyst. The maximum photodegradation was found at neutral pH, 6.25 ppm concentration of dye solution, 800 mg/L amount of photocatalyst and 120 min irradiation of visible light. Kinetics study was investigated for the photodegradation of Rose Bengal dye and found first order kinetics. The coating of PAni and GO has enhanced the photocatalytic activity of Titania. Hence $TiO_2$/PAni and $TiO_2$/PAni/GO is the efficient photocatalyst for the degradation of Rose Bengal dye than pure $TiO_2$.

## IV. ACKNOWLEDGEMENT

We thanks for financial assistance to UGC, Government of India is acknowledged. The authors also acknowledge the support provided by the BabasahebBhimraoAmbedkar University, Lucknow, India

## REFERENCES

[1]. Y. Li, Y. Yu, L. Wu, J. Zhi, Processable Polyaniline/Titanianocomposites with good photocatalytic and conductivity properties prepared via peroxo-titanium complex catalyzed emulsion polymerization approach, Applied Surface Science, 273, 2013, 135-143
[2]. H.M. Moghaddam, S. Nasirian, Hydrogen gas sensing feature of Polyaniline/Titania (rutile) nanocomposites at environmental conditions, Applied Surface Science, 317, 2014, 117-124
[3]. H. Huang, M. Gan, M. Li, L. Yu, H. Hu, F. Yang, Y. Li, C. Ge, Fabrication of Polyaniline/Graphen oxide/ Titania nanotube arrays nanocompositesand their application in supercapacitors, Journal of Alloys and Compounds, 630, 2015, 214-221
[4]. S.H. Nimkar, S.P. Agrawal, S.B. Kondawar, Fabrication of ElectrospunNanofibers of Titanium Dioxide Intercalated polyaniline nano-composites for $CO_2$ Gas SensorProcedia Materials Science, 10, 2015, 572-579
[5]. S. Nasirian, H. M. Moghaddam, Effect of different titania phases on the hydrogen gas sensing feature of polyaniline /$TiO_2$ nanocomposite, Polymer, 55, 2014, 1866-1874
[6]. C. Su, Environmental implications and applications of engineered nanoscale magnetite and its hybrid nanocomposites: A review of recent literature, Journal of Hazardous Materials, 322, 2017, 48-84
[7]. D.C. Clifford, C.E. Castano, J.V. Rojas, Supported transition metal nanomaterials: nanocomposites synthesized by ionizing radiation, Radiation Physics and Chemistry, 132, 2017, 52-64
[8]. S. Nasirian, H. M. Moghaddam, Hydrogen gas sensing base on polyaniline /anatase titania nanocomposite, Int. Journal of Hydrogen Energy, 39, 2014, 630-642
[9]. L. Su, Y. Li, X. Gan, Experimental study on synthesizing$TiO_2$ nanotube/polyaniline (PANI) nanocomposites and their thermoelectric and photosensitive property characterization, Composites Part B: Engineering, 43, 2012, 170-182
[10]. Y. Wu, X. Zhang, S. Li, X. Lv, Y. Cheng, X. Wang, Microbial biofuel cell operating effectively through carbon nanotube blended with gold titania nanocomposites modified electrode, ElectrochimicaActa, 109, 2013, 328-332
[11]. H. Sawada, T. Tsuzuki-ishi, T. Kijima, J. Kawakami, M. Iizuka, M. Yoshida, Controlling photochromism between fluoroalkyl end-capped oligomer/polyaniline and N,N′-diphenyl-1,4-phenylenediamine nanocomposites induced by UV-light-responsive titanium oxide nanoparticles, J. of Colloid and Interface Science, 359, 2011, 461-466
[12]. C.T. Fleaca, F. Dumitrache, I. Morjan, A.-M. Niculescu, I. Sandu, A. Ilie, I. Stamatin, A. Iordache, E. Vasile, G. Prodan, Synthesis and characterization of polyaniline –Fe@C magnetic nano-composites powder, App. Sur. Sci.,374, 2016, 213-221
[13]. M.C. Arenas, L. Fernando Rodríguez-Núnez, Domingo Rangel, Omar Martínez-Álvarez, Claudia Martínez-Alonso, V.M. Castaño, Simple one-step ultrasonic synthesis of anatase titania/polypyrrole nanocomposites, Ultra. Sonoche., 20, 2013, 777-784
[14]. M. R. Karim, K. T. Lim, M. S. Lee, K. Kim, J. H. Yeum, Sulfonated polyaniline –titanium dioxide nanocomposites synthesized by one-pot UV-curable polymerization method, Synthetic Metals, 159, 2009, 209-213
[15]. S. Xie, M. Gan, L. Ma, Z. Li, J. Yan, H.Yin, X. Shen, F. Xu, J. Zheng, J. Zhang, J. Hu, Synthesis of polyaniline-titania nanotube arrays hybrid composite via self-assembling and graft polymerization for supercapacitor application, ElectrochimicaActa, 120, 2014, 408-415.
[16]. Vinuth M, Naik HSB, Vinoda BM, Pradeepa SM, Arun KG, et al. (2016) Rapid Removal of Hazardous Rose Bengal Dye Using Fe(III)–Montmorillonite as an Effective Adsorbent in Aqueous Solution. J Environ Anal Toxicol 6: 355. doi:10.4172/2161-0525.1000355
[17]. Sarmah, S. and Kumar, A. (2011) Photocatalytic Activity of Polyaniline-TiO2 Nanocomposites. Indian Journal of Physics, 85, 713-726.
[18]. J.Kaur, S.Singha, Heterogeneous photocatalytic degradation of rose bengal: Effect of operational parameters,Physica B: Condensed Matter, Volume 450, 1 October 2014, Pages 49-53

[19]. G. K.Pradhan, D.Padhi, and K.Parida, Fabrication of #-Fe2O3 Nanorod/RGO composite: A novel hybrid photocatalyst for phenol degradation, Appl. Mater. Interfaces 2013, 5, 9101–9110
[20]. M.R. Nabid, M. Golbabaee, A. B.Moghaddam , R.Dinarvand , R.Sedghi, Polyaniline/TiO2 Nanocomposite: Enzymatic Synthesis and Electrochemical Properties Int. J. Electrochem. Sci., 3 (2008) 1117 – 1126
[21]. X.Li , D. Wang, G. Cheng , Q.Luo, J. An , Y. Wang, Preparation of polyaniline-modified TiO2 nanoparticles and their photocatalytic activity under visible light illumination, Applied Catalysis B: Environmental 81 (2008) 267–273
[22]. S. B.Gajbhiye, Photocatalytic Degradation Study of Methylene Blue Solutions and Its Application to Dye Industry Effluent, International Journal of Modern Engineering Research (IJMER), Vol.2, Issue.3, May-June 2012 pp-1204-1208
[23]. Z. Carmen and S. Daniela (2012). Textile Organic Dyes – Characteristics, Polluting Effects and Separation/Elimination Procedures from Industrial Effluents – A Critical Overview, Organic Pollutants Ten Years After the Stockholm Convention - Environmental and Analytical Update, Dr. Tomasz Puzyn (Ed.), InTech, DOI: 10.5772/32373.
[24]. R. Arora, U. K. Mandal, P. Sharma, A. Srivastav, Synthesis and Thermal Properties of polyaniline-TiO2nanocomposites PVA Based Film, Materials Today: Proceedings, 2, 2015, 2215-2225
[25]. B. Wang, C. Liu, Y. Yin, S. Yu, K. Chen, P. Liu, B. Liang, Double template assisting synthesized core–shell structured titania/polyaniline nanocomposites and its smart electrorheological response, Composites Science and Technology, 86, 2013, 89-100
[26]. H. Wang, L. Ma, M. Gan, T. Zhou, X. Sun, Wenqin. Dai, H. Wang, S. Wang, Fabrication of polyaniline /urchin-like mesoporous $TiO_2$ spheres nanocomposites and its application in supercapacitors, ElectrochimicaActa, 163, 2015, 232-237
[27]. S. Kango, S. Kalia, A. Celli, J. Njuguna, Y. Habibi, R. Kumar, Surface modification of inorganic nanoparticles for development of organic–inorganic nanocomposites -A review, Progress in Polymer Science, 38, 2013, 1232-1261
[28]. S. Chowdhury, R. Balasubramanian, Graphene / semiconductor nanocomposites (GSNs) for heterogeneous photocatalyticdecolorization of wastewaters contaminated with synthetic dyes: A review, Applied Catalysis B: Environmental, 160–161, 2014, 307-324
[29]. S. Al-Hussaini, R. K. Eltabie, M.E.E. Rashad, One-pot modern fabrication and characterization of $TiO_2$@terpoly(aniline, anthranilic acid and o-phenylenediamine) core-shell nanocomposites viapolycondensation, Polymer, 101, 2016, 328-337
[30]. P.T. Patil, R.S. Anwane, S.B. Kondawar, Development of Electrospun polyaniline /ZnO Composite Nanofibers for LPG Sensing, Procedia Mat. Sci., 10, 2015, 195-204
[31]. C. Lai, G.R. Li, Y.Y. Dou, X.P. Gao, Mesoporous polyaniline or polypyrrole/anatase $TiO_2$ nanocomposites as anode materials for lithium-ion batteries, ElectrochimicaActa, 55, 2010, 4567-4572
[32]. S. Bhandari, N.K. Singha, D. Khastgir, Synthesis of graphene-like ultrathin polyaniline and its post-polymerization coating on nanosilica leading towards superhydrophobicity of composites, Chemical Engineering Journal, In Press, Corrected Proof, Available online 8 November 2016
[33]. A. Aashish, R. Ramakrishnan, J.D. Sudha, M. Sankaran, G. Krishnapriya, Self-assembled hybrid polyvinylcarbazole–titania nanotubes as an efficient photoanode for solar energy harvesting, Solar Energy Materials and Solar Cells, 151, 2016, 169-178
[34]. Kumar, A. Bansal, B. Behera, S. L. Jain, S.S. Ray, Ternary hybrid polymeric nanocomposites through grafting of polystyrene on graphene oxide-$TiO_2$ by surface initiated atom transfer radical polymerization (SI-ATRP), Materials Chemistry and Physics, 172, 2016, 189-196
[35]. G.K. Prasad, T. Takei, Y. Yonesaki, N. Kumada, N. Kinomura, Hybrid nanocomposites based on $NbWO_6$ nanosheets and polyaniline, Materials Letters, 60, 2006, 3727-3730
[36]. H. Wang, J. Lin, Z. X. Shen,polyaniline (PAni) based electrode materials for energy storage and conversion, Journal of Science: Adv. Mat. and Devices, 1, 2016, 225-255
[37]. L. Zhang, P. Liu, Z. Su, Preparation of PANI–$TiO_2$ nanocomposites and their solid-phase photocatalytic degradation, Pol. Degra. and Stability, 91, 2006, 2213-2219
[38]. J.A.V Albelda, A. Uzunoglu, G. N.C. Santos, L. A. Stanciu, Graphene-titanium dioxide nanocomposites based hypoxanthine sensor for assessment of meat freshness, Biosensors and Bioelectronics, 89, 2017, 518-524
[39]. S. Ameen, M.S. Akhtar, Y.S. Kim, H.S. Shin, nanocomposites of poly(1-naphthylamine)/$SiO_2$ and poly(1-naphthylamine)/$TiO_2$: Comparative photocatalytic activity evaluation towards methylene blue dye,App. Cat. B: Env., 103, 2011, 136-142
[40]. S.C. Tjong, Structural and mechanical properties of polymer nanocomposites, Materials Science and Engineering: R: Reports, 53, 2006, 73-197
[41]. R. Arora, U.K. Mandal, P. Sharma, A. Srivastav, Effect of fabrication technique on microstructure and electrical conductivity of polyaniline-TiO2-PVA composite material, Procedia Materials Science, 6, 2014, 238-243
[42]. S. Sultana, M. Rafiuddin, M. Z. Khan, K. Umar, Synthesis and characterization of copper ferrite nanoparticles doped polyaniline, J. of Al. & Comp., 535, 2012, 44-49
[43]. G. Zhou, D. Wang, F. Li, L. Zhang, Z. Weng, H. Cheng, The effect of carbon particle morphology on the electrochemical properties of nanocarbon/polyaniline composites in supercapacitors, New Carbon Materials, 26, 2011, 180-186
[44]. A. Zięba, A. Drelinkiewicz, E.N. Konyushenko, J. Stejskal, Activity and stability of polyaniline -sulfate-based solid acid catalysts for the trans esterification of triglycerides and esterification of fatty acids with methanol, Applied Catalysis A: General, 383, 2010, 169-181
[45]. H. Liang, X. Li, Visible-induced photocatalytic reactivity of polymer–sensitized titania nanotube films, Applied Catalysis B: Environmental, 86, 2009, 8-17
[46]. X. Tang, M. Tian, L. Qu, S. Zhu, X. Guo, G. Han, K. Sun, X. Hu, Y. Wang, X. Xu, Functionalization of cotton fabric with graphene oxide nanosheet and polyaniline for conductive and UV blocking properties, Synthetic Metals, 202, 2015, 82-88
[47]. X. Wang, S. Tang, C. Zhou, J. Liu, W. Feng, Uniform $TiO_2$–PANIcomposite capsules and hollow spheres, Synthetic Metals, 159, 2009, 1865-1869
[48]. G.A. Epling, C. Lin, Photoassisted bleaching of dyes utilizing TiO2 and visible light, Chemosphere 46 (2002) 561–570.
[49]. M.M. Ba-Abbad, A.A.H. Kadhum, A.B. Mohamad, M.S. Takriff, K. Sopian, Synthesis and catalytic activity of $TiO_2$ nanoparticles for photochemical oxidation of concentrated chlorophenols under direct solar radiation, Int. J. Electrochem. Sci 7 (2012), 4871–4888.
[50]. S. Yang, X. Yang, X. Shao, R. Niu, L. Wang, Activated carbon catalyzedpersulfate oxidation of Azo dye acid orange 7 at ambient temperature, J. Haz. Mater. 186 (2011) 659–666.

[51]. H. Lachheb, E. Puzenat, A. Houas, M. Ksibi, E. Elaloui, C. Guillard, J.M. Herrmann, Photocatalytic degradation of various types of dyes (Alizarin S, Crocein Orange G, Methyl Red, Congo Red, Methylene Blue) in water by UV-irradiated titania, Appl. Catal. B: Environ. 39 (2002) 75–90.
[52]. A.E. Gary and C. Lin, Investigation of retardation effects on the titanium dioxide photodegradation systemChemosphere, 46 (2002)937-944.
[53]. M. Toyoda, T. Yano, B. Tryba, S. Mozia, T. Tsumura, and M. Inagaki,Preparation of carbon-coated Magneli phases $Ti_nO_{2n-1}$ and their photocatalytic activity under visible light, Applied Catalysis B: Environmental, 88 (2009) 160-164.
[54]. R. Byberg, J. Cobb, L.D. Martin, R.W. Thompson, T.A. Camesano, O. Zahraa, M.N. Pons, Comparison of photocatalytic degradation of dyes in relation to their structure, Environ. Sci. Pollut. Res. 20 (2013) 3570–3581.
[55]. J.D. Kwon, P.H. Kim, J.H. Keum, J.S. Kim, Polypyrrole/titania hybrids: synthetic variation and test for the photovoltaic materials. Sol Energy Mater Sol Cells 83 (2004) 311–321.
[56]. L. Zhang, P. Liu, Z. Su, Preparation of PANI–$TiO_2$ nanocomposites and their solid-phase photocatalytic degradation, Poly. Degra. and Stability, 91, 2006, 2213-2219
[57]. J. Li, L. Zhu, Y. Wu, Y. Harima, A. Zhang, H. Tang, Hybrid composites of conductive polyaniline and nanocrystalline titanium oxide prepared via self-assembling and graft polymerization, Polymer, 47, 2006, 7361-7367
[58]. Xiaobo, S.S. Mao, Titanium dioxide nanomaterials: synthesis, properties, modifications and application, Chem. Rev., 107 (2007), pp. 2891–2906
[59]. U. Diebold, The surface science of titanium dioxide, Surf. Sci. Rep., 48 (2003), pp. 53–229
[60]. X. Li, Z. Wang, X. Li, G. Wang, Synthesis of a super-hydrophilic conducting polyaniline/titanium oxide hybrid with a narrow pore size distribution, Appl. Surf. Sci., 258 (2012), pp. 4788–4793
[61]. S. Deivanayaki, V. Ponnuswamy, S. Ashokan, P. Jayamurugan, R. Mariappan, Synthesis and characterization of $TiO_2$-doped polyanilinenanocomposites by chemical oxidation method, Mater. Sci. Semicond. Process., 16 (2013), pp. 554–559
[62]. A. Katoch, M. Burkhart, T. Hwang, S.S. Kim, Synthesis of polyaniline/$TiO_2$ hybrid nanoplates via a sol–gel chemical method, Chem. Eng. J., 192 (2012), pp. 262–268
[63]. S. Deivanayaki, V. Ponnuswamy n , S. Ashokan, P. Jayamurugan, R. Mariappan, Synthesis and characterization of TiO2-doped Polyanilinenanocomposites by chemical oxidation method Materials Science in Semiconductor Processing 16 (2013) 554–559
[64]. E. Kordouli, K. Bourikas, A. Lycourghiotis, C. Kordulis, The mechanism of azo-dyes adsorption on the titanium dioxide surface and their photocatalytic degradation over samples with various anatase/rutile ratios. Catal Today 252, (2015) 128–135
[65]. S.K. Kansal, M. Singh, D. Sud, Studies on photodegradation of two commercial dyes in aqueous phase using different photocatalysts. J Hazard Mater 141 (2007) 581–590 11.
[66]. E. Vulliet, J.M. Chovelon, C. Guillard, J.M. Herrmann, Factors influencing the photocatalytic degradation of sulfonylurea herbicides by TiO2 aqueous suspension, J. Photochem. Photobiol. A: Chem. 159 (2003), 71–79.
[67]. I.K. Konstantinou, T.A. Albanis TiO2-assisted photocatalytic degradation of azo dyes in aqueous solution: kinetics and mechanistic investigations. A review. ApplCatal B 49 (2004) 1–14
[68]. R.W. Matthews, Kinetics of photocatalytic oxidation of organic solutes over titanium dioxide, J. Catal. 111 (1988), 264–272.
[69]. M. Vautier, C. Guillard, J.M. Herrmann, Photocatalytic degradation of dyes in water: Case study of Indigo and of Indigo Carmine, J. Catal. 201 (2001), 46–59.
[70]. R.W. Matthews, Kinetics of photocatalytic oxidation of organic solutes over titanium dioxide, J. Catal. 111 (1988), 264–272.

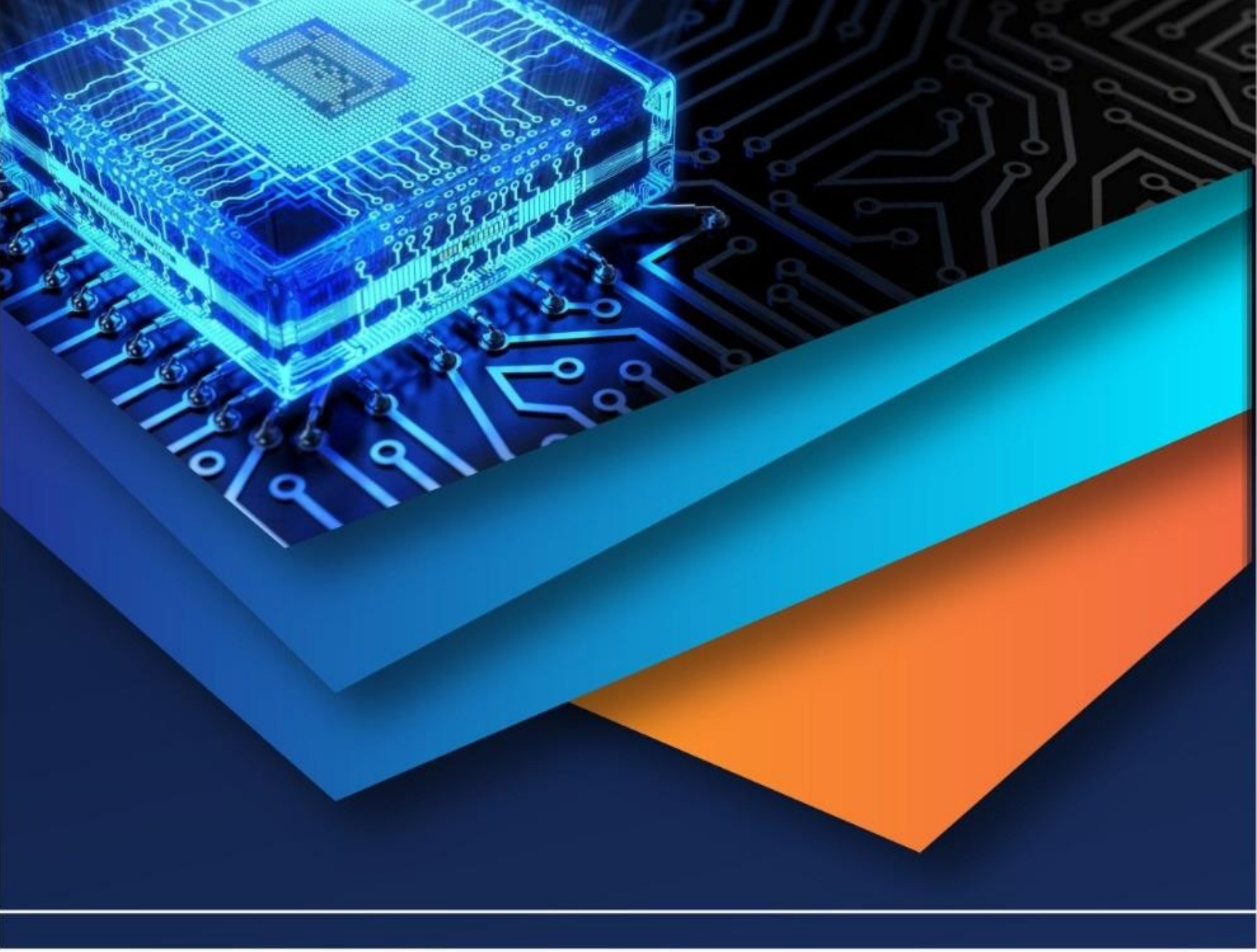

10.22214/IJRASET

45.98

IMPACT FACTOR: 7.129

IMPACT FACTOR: 7.429

# INTERNATIONAL JOURNAL FOR RESEARCH

IN APPLIED SCIENCE & ENGINEERING TECHNOLOGY